Development of a Model-Based Nested Controller for Electrohydraulic Servos

Ioannis Davliakos[1] and Evangelos Papadopoulos[2 3], *Senior Member, IEEE*

***Abstract*—In this paper, a tracking controller for electrohydraulic servosystems is developed that includes a fast model-based force tracking loop. Full rigid body and electrohydraulic models, including servovalve models are employed and described by a set of integrated system equations. The control analysis is based on a non-linear input-output linearization control approach. The control law is augmented with a PD part, responsible for the exponential convergence of the tracking error to zero. The proposed methodology is illustrated by a detailed example.**

I. Introduction

The combination of hydraulics science with servo control, or *hydrotronics*, has given new thrust to hydraulics applications, [1]. The main reasons why hydrotronics are preferred to electromechanical drives in some industrial and mobile applications, include their ability to produce large forces at high speeds, their high durability and stiffness, and their rapid response [2].

Control techniques are used to compensate for the nonlinearities of electrohydraulic servosystems. Nonlinear adaptive control techniques for hydraulic servosystems have been proposed by researchers assuming linearization [3] and backstepping [4], approaches.

Hydraulic systems differ from electromechanical ones, in that the force or torque output is not proportional to actuator current and therefore, hydraulic actuators cannot be modeled as force/ torque sources. As a result, controllers that have been designed for robot control, assuming the capability of setting actuator force/ torque, cannot be used here. To be able to use such controllers, a hydraulic actuator should be able first to apply a desired force.

A robust force controller design based on the nonlinear Quantitative Feedback Theory, has been implemented on an industrial hydraulic actuator, taking into account system and environmental uncertainties, [5].

Force control of hydraulic servosystems has been proposed, such as a neural network adaptive control [6], in which an on line system parameter estimation scheme is used, and an *H-infinity* approach is issued [7], where a robustly force controller is applied on a double-acting symmetric servocylinder. Further, impedance controllers have been studied and implemented on teleoperated hydraulic servosystems for heavy duty works [8], as well as on hydro-elastic actuators [9].

Most of the previous work associated with force/pressure tracking control has focused on electrohydraulic servoactuators and has been developed based on Lyapunov analysis [10]-[12]. A model based controller of hydraulically actuated manipulators has been studied, but the feedforward controller terms were calculated using desired and not actual positions [13]. Early efforts on an other model based force and motion control analysis has been developed with satisfactory tracking response, [14].

In this paper, a tracking controller for electrohydraulic servosystems is developed that includes a fast model-based force tracking loop. Dynamic models are proposed that describe the rigid body equations of motion and the hydraulic dynamics. Friction and leakages of hydraulic elements are included in the full electrohydraulic model. A model based force controller is developed, which is augmented by a PD part, responsible for the exponential convergence of the tracking error to zero. A case study of a servomechanism with one degree of freedom is examined.

II. Electrohydraulic Servosystem Modeling

In this section, the dynamic modeling of high performance electrohydraulic servocylinders is presented briefly. An electrohydraulic servosystem consists of a servomechanism, including a servovalve, a servoactuator, a controller, a mechanical load and a hydraulic power supply. Next, simple models of major components are described.

A. Hydraulic Dynamics

An ideal single rod hydraulic cylinder is described by

$$Q_r = A_r \dot{x}_p , \quad r = 1,2 \tag{1a}$$

$$p_1 A_1 - p_2 A_2 = F_p \tag{1b}$$

where Q_r are the flows through its two chamber ports, p_1 ,

[1] I. Davliakos is with the National Technical University of Athens, Greece (e-mail: gdavliak@central.ntua.gr).

[2] E. Papadopoulos is with the National Technical University of Athens (NTUA), Greece (corresponding author, phone: +(30) 210-772-1440; fax: +(30) 210-772-1455; e-mail: egpapado@central.ntua.gr).

[3] Support of this work by the Hellenic General Secretariat for Research and Technology (EPAN M. 4.3.6.1) and the NTUA Senator Committee of Basic Research, Programme "Protagoras", R.C. No. 10, is acknowledged.

p_2 are the chamber pressures, A_1 is the piston side area, A_2 is the rod side area, x_p is the piston displacement and F_p is the piston output force. A real cylinder model also includes chamber oil compressibility, friction and other effects. However, these can be neglected at an initial stage.

Control of hydraulic systems is achieved through the use of servovalves. Only the resistive effect of a valve is considered here, since their natural frequency is much higher that of the hydraulics and mechanical load. It is also assumed than that the geometry of the valve is ideal, e.g. sharp edges, zero cross leakages [16]. The valve elemental (orifice) equations for the two symmetrical orifices is

$$\Delta p_{v,k} = C_R Q_{v,k} \left| Q_{v,k} \right| , \quad k = 1,2 \tag{2}$$

where $\Delta p_{v,k}$ is the valve orifice pressure drop, $Q_{v,k}$ is the corresponding flow through an orifice and C_R is a coefficient, which depends on the orifice area S, the discharge coefficient C_d and the fluid mass density ρ,

$$C_R = 0.5 \rho C_d^{-2} S^{-2} \tag{3}$$

For short tubes and turbulent flow, the C_d is as function of the Reynolds number and valve geometry. However, it can be approximated by a constant, [16].

The full servovalve model that is studied consists of four symmetric and matched servovalve orifices make up a four-legged flow path of four nonlinear resistors modulated by the input voltage and thereby the servovalve is modeled as the hydraulic equivalent of a Wheatstone bridge, see Fig. 1. When flow passes through the orifices 1 and 3 (path $P \to A \to B \to T$), flow leakages exist in the valve orifices 2 and 4. Respectively, when flow passes through the path $P \to B \to A \to T$, flow leakages exist in the valve orifices 1 and 3. This model is described by

$$Q_{v1} = f_1(i)\sqrt{p_s - p_1}, \quad Q_{v3} = f_2(i)\sqrt{p_2 - p_T} \tag{4a}$$

$$Q_{v2} = g_1(i)\sqrt{p_s - p_2}, \quad Q_{v4} = g_2(i)\sqrt{p_1 - p_T} \tag{4b}$$

where p_s and p_T are the power supply and return pressure of the servosystem, respectively, i is the servovalve motor current (control command), and $f_1(i)$, $f_2(i)$, $g_1(i)$ and $g_2(i)$ are servovalve nonlinear orifice conductances, functions of the servovalve motor current. Because of servovalve symmetry, the current functions are given by

$$f_1(i) = g_1(i) = f_2(-i) \tag{5a}$$

$$f_2(i) = g_2(i) = f_1(-i) \tag{5b}$$

In the case of an ideal hydraulic cylinder with a double rod, the two areas A_1 and A_2 are equal and therefore, (1) is simplified further.

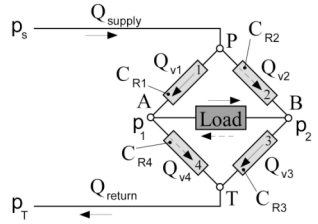

Fig. 1. Schematic model of servovalve.

B. Mechanical Load Dynamics

The servomechanism equation of motion is given by

$$\mathbf{M}(\boldsymbol{q})\ddot{\boldsymbol{q}} + \boldsymbol{V}(\boldsymbol{q},\dot{\boldsymbol{q}}) + \boldsymbol{G}(\boldsymbol{q}) + \boldsymbol{F}_{fr}(\dot{\boldsymbol{q}}) = \boldsymbol{\tau} \tag{6}$$

where $\boldsymbol{q}$ is the $n \times 1$ vector of generalized coordinates, $\mathbf{M}(\boldsymbol{q})$ is the $n \times n$ positive definite mass matrix, the $n \times 1$ vector $\boldsymbol{V}(\boldsymbol{q},\dot{\boldsymbol{q}})$ represents forces/torques arising from centrifugal and Coriolis forces, the $n \times 1$ vector $\boldsymbol{G}(\boldsymbol{q})$ represents torques due to gravity, $\boldsymbol{F}_{fr}(\dot{\boldsymbol{q}})$ is the $n \times 1$ vector of the forces / torques due to friction and $\boldsymbol{\tau}$ is the $n \times 1$ vector of actuator joint torques.

A number of methods exists, that model the friction vector $\boldsymbol{F}_{fr}(\dot{\boldsymbol{q}})$ [17]. A widely used method suggests,

$$\boldsymbol{F}_{fr}(\dot{\boldsymbol{q}}) = \boldsymbol{F}_{v}(\dot{\boldsymbol{q}}) + \boldsymbol{F}_{c}(\dot{\boldsymbol{q}}) \tag{7}$$

where $\boldsymbol{F}_{v}(\dot{\boldsymbol{q}})$ and $\boldsymbol{F}_{c}(\dot{\boldsymbol{q}})$ are the viscous and Coulomb friction vector respectively, with elements,

$$F_{v,j}(\dot{q}_j) = b_j \dot{q}_j, \quad j = 1,...,n \tag{8a}$$

$$F_{c,j}(\dot{q}_j) = F_{c0,j} sign(\dot{q}_j), \quad j = 1,...,n \tag{8b}$$

where q_j is the j generalized coordinate, b_j is the j parameter for viscous friction, $F_{c0,j}$ is the j parameter for Coulomb friction and

$$sign(\dot{q}_j) = \begin{cases} +1, & \dot{q}_j > 0 \\ 0, & \dot{q}_j = 0 \\ -1, & \dot{q}_j < 0 \end{cases} \tag{9}$$

If static friction is added to this model, the classical friction model is complete. According to this model, during stick, friction force can be modeled as a function of external force, with elements,

$$F_{s,j} = \begin{cases} F_{ext,j}, & \left|F_{ext,j}\right| < F_{s0,j}, \dot{q}_j = 0, \ddot{q}_j = 0 \\ F_{s0,j} sign(F_{ext,j}), & \left|F_{ext,j}\right| > F_{s0,j}, \dot{q}_j = 0, \ddot{q}_j \neq 0 \end{cases} \tag{10}$$

where $F_{ext,j}$ is the j parameter for external force and $F_{s0,j}$ is the j parameter for breakaway force, which is the limit between static and kinetic friction.

C. Integrated System Equations

Hydraulic actuation dynamics can be written using a systems approach, such as the Linear Graph or Bond Graph methods. This results in a set of nonlinear state space equations. To integrate these models to the mechanical load dynamics, one needs to provide expressions transforming pressure differences to forces, see (1b), and velocities to flows, see (1a). In general, hydraulic and load dynamics are described by nonlinear equations,

$$\begin{aligned} \dot{\boldsymbol{x}} &= \boldsymbol{f}(\boldsymbol{x}) + \boldsymbol{g}(\boldsymbol{x})\boldsymbol{u} \\ \boldsymbol{y} &= \boldsymbol{h}(\boldsymbol{x}), \qquad \boldsymbol{x_0} = \boldsymbol{x}(t_0) = \boldsymbol{x}(0) \end{aligned} \tag{11}$$

where $\boldsymbol{x}$ is a state vector, $\boldsymbol{u}$ is the input column vector, $\boldsymbol{y}$ is the output column vector and $\boldsymbol{f}(\boldsymbol{x})$, $\boldsymbol{g}(\boldsymbol{x})$ and $\boldsymbol{h}(\boldsymbol{x})$ are nonlinear functions of appropriate dimensions.

III. Single Dof Electrohydraulic Servomechanism

A. Dynamic Modeling

In this section, the dynamic model of one-degree-of-freedom electrohydraulic servomechanism is developed. This servo is to be used as an actuator in a robotic Stewart type mechanism [18], i.e. a six dof closed kinematic chain mechanism consisting of a fixed base and a movable platform with six linear actuators supporting it. The one dof mechanism is illustrated schematically in Fig. 2.

The angles of inclination of the actuator θ and the load φ shown in Fig. 2 can be expressed as function of the displacement of the actuator, x_p. Applying the Lagrange formulation, the equation of motion is written as

$$M(x_p)\ddot{x}_p + V(x_p,\dot{x}_p) + G(x_p) + F_{fr}(\dot{x}_p) = F_p \tag{12}$$

where $M(x_p)$ is a positive definite function, which represents the variable apparent mass of the mechanism, as seen by the actuator, $V(x_p,\dot{x}_p)$ contains the Coriolis and centrifugal terms, $G(x_p)$ represents the gravity term (see Appendix), F_p is the force applied to the mechanical load and $F_{fr}(\dot{x}_p)$ is the friction term given by

$$F_{fr}(\dot{x}_p) = b\dot{x}_p + F_{c0}\,sign(\dot{x}_p) + F_s \tag{13}$$

where

$$F_s = \begin{cases} F_{ext}, & |F_{ext}| < F_{s0},\ \dot{x}_p = 0,\ \ddot{x}_p = 0 \\ F_{s0}\,sign(F_{ext}), & |F_{ext}| > F_{s0},\ \dot{x}_p = 0,\ \ddot{x}_p \neq 0 \end{cases} \tag{14}$$

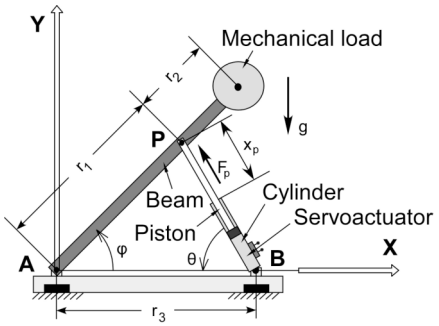

Fig. 2. Schematic view of the one DOF servomechanism model.

The hydraulics equations of the servomechanism shown in Fig. 3 are described by (1)-(5). One of the most important characteristics is the servovalve characteristic, $Q_v - \Delta p_v$, described in Section II. The flow through the cylinder and the piston output force applied to the load are given by (1a) and (1b) correspondingly. The pressure drop at the servovalve is expressed by (2), neglecting auxiliary elements pressure drops.

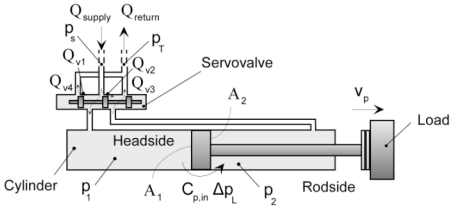

Fig. 3. Schematic model of hydraulic servoactuator.

The linear graph of the full model of the hydraulic servosystem is depicted in Fig. 4. The application of continuity and compatibility laws, along with individual elements equations, leads to a set of eight nonlinear first order differential equations as follows,

$$\dot{p}_1 = [Q_{I,l1} - Q_{v2} - Q_{v4} - C_{p,in}(p_1 - p_2) - A_1 v_p]C_1^{-1} \tag{15a}$$

$$\dot{p}_2 = [Q_{v2} + Q_{v4} - Q_{I,l2} + C_{p,in}(p_1 - p_2) - A_2 v_p]C_2^{-1} \tag{15b}$$

$$\dot{p}_{C,l1} = [(p_s - p_{C,l1})/R_{l1} - Q_{I,l1}]C_{l1}^{-1} \tag{15c}$$

$$\dot{p}_{C,l2} = [Q_{I,l2} - (p_{C,l2} - p_T)/R_{l2}]C_{l2}^{-1} \tag{15d}$$

$$\dot{Q}_{I,l1} = [p_{C,l1} - p_1 - C_{R1}Q_{v1}|Q_{v1}|]I_{l1}^{-1} \tag{15e}$$

$$\dot{Q}_{I,l2} = [p_2 - p_{C,l2} - C_{R3}Q_{v3}|Q_{v3}|]I_{l2}^{-1} \tag{15f}$$

$$\dot{v}_p = M^{-1}(x_p)[A_1 p_1 - A_2 p_2 - V(x_p,\dot{x}_p) - G(x_p) - F_{fr}(\dot{x}_p)] \tag{15g}$$

$$\dot{x}_p = v_p \tag{15h}$$

where $Q_{I,l1}$, $Q_{I,l2}$ are the flows in hydraulic power and return line correspondingly, $p_{C,l1}$, $p_{C,l2}$ are respectively the

pressures of hydraulic power and return line regarding with the lines' capacitances, I_{l1}, R_{l1} and C_{l1} are the inertance, resistance and capacitance of hydraulic power line respectively, I_{l2}, R_{l2} and C_{l2} are the inertance, resistance and capacitance of hydraulic return line respectively, C_1, C_2 are the fluid capacitance in the servoactuator chambers and $C_{p,in}$ is the internal leakage coefficient of piston.

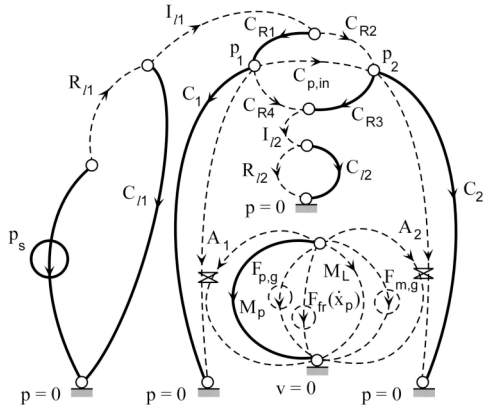

Fig. 4. Full linear graph of the one DOF servomechanism model.

The four variables $p_{C,l1}$, $p_{C,l2}$, $Q_{I,l1}$, and $Q_{I,l2}$ are related to hydraulic line response but are not part of the control scheme. However, the dynamics associated with these are stable, see (15).

The output of the system is the force acting on the load mass and beam, and is given by

$$y = F_m = M_m(x_p)\,\ddot{x}_p + V_m(x_p,\dot{x}_p) + G_m(x_p) \tag{16}$$

where $M_m(x_p)$ is the part of $M(x_p)$, which represents the variable apparent mass of the load and beam, $V_m(x_p,\dot{x}_p)$ is the part of $V(x_p,\dot{x}_p)$, which contains velocity terms and $G_m(x_p)$ is the part of $G(x_p)$, which represents gravity term of the load mass and beam. The integrated system equations, see (11), are given by (15a-b), (15g-h), and (16).

B. Force Controller

In electromechanical systems, the force acting on moving masses is proportional to actuator current. This simplifies their control laws and allows one to achieve second order error dynamics converging exponentially to zero. However, a simple relationship between force and current does not exist in electrohydraulic systems. Despite of this, we are interested in studying whether such a system can be described by error dynamics such as

$$\ddot{e}_p + K_v\dot{e}_p + K_p e_p = 0 \tag{17}$$

where $e_p = x_{p,des} - x_p$ is the position error and K_p and K_v are control gains. To this end, a relationship between the force acting on the load and the control input, is sought.

Assuming that (17) have been achieved, this equation is solved for $\ddot{x}_p$ which is then substituted in (16). The result is a force that must be applied by the piston, so that the error of the load motion is governed by (17). Therefore, the desired actuator force is given by,

$$\begin{aligned} F_{m,des} = M_m(x_p)[\ddot{x}_{p,des} + K_v(\dot{x}_{p,des} - \dot{x}_p) + \\ + K_p(x_{p,des} - x_p)]V_m(x_p,\dot{x}_p) + G_m(x_p) \end{aligned} \tag{18}$$

To generate a relationship between force and current, the output (16) is differentiated up to the point that the input does not explicitly appear. Differentiating once, (16) yields

$$\dot{y} = \dot{F}_m = \dot{F}_m(x_p,\dot{x}_p,\dot{v}_p,\ddot{v}_p) \tag{19}$$

Differentiating the piston acceleration, (15g), yields

$$\ddot{v}_p = \ddot{v}_p(x_p,v_p,p_1,p_2) \tag{20}$$

Taking into account (15a-h), (19) takes the form

$$\dot{F}_m = \dot{F}_m(x_p,v_p,p_1,p_2) \tag{21}$$

Further, the servovalve orifice conductances are assumed to be linear functions of the input current. Therefore, the flows through the orifices of the servovalve are written as

$$Q_{v1} = (K_1 i + K_{0,1})\sqrt{p_s - p_1},\; Q_{v3} = (K_2 i + K_{0,2})\sqrt{p_2 - p_T} \tag{22a}$$

$$Q_{v2} = (K_1 i + K_{0,1})\sqrt{p_s - p_2},\; Q_{v4} = (K_2 i + K_{0,2})\sqrt{p_1 - p_T} \tag{22b}$$

where K_1, $K_{0,1}$, K_2 and $K_{0,2}$ are positive constants, which correspond to the main and leakage valve flow path.

Substituting (22a) and (22b) into (21), yields

$$\dot{F}_m = \hbar_1(x_p,v_p,p_1,p_2)\cdot i + \hbar_2(x_p,v_p,p_1,p_2) \tag{23}$$

where $\hbar_1(x_p,v_p,p_1,p_2)$ and $\hbar_2(x_p,v_p,p_1,p_2)$ are nonlinear functions of the state variables. Eq. (23) shows that one can find a relationship between the current and the derivative of the force and not the force itself, as in electric actuators.

Also, (23) suggests that one can design a controller that will allow the output force to converge to the desired one according to the following first order error equation

$$\dot{e}_f + K_f e_f = 0 \tag{24}$$

where K_f is a gain and $e_f = F_{m,des} - F_m$ is the force error.

Substituting (23) in (24), a control law that computes the servovalve current results:

$$i = [\dot{F}_{m,des} + K_f(F_{m,des} - F_m) - \hbar_2]\,\hbar_1^{-1} \tag{25}$$

Note that this control law requires feedback of both the

position and velocity error, included in $F_{m,des}$, as well as of the force developed by the actuator. A detailed look shows that the controller is made of two nested loops, a faster internal force loop and a slower external position loop, see Fig. 5. An advantage is that it does not require an estimate of the piston jerk or of the derivative of the force F_m, which are problematic in the presence of noise.

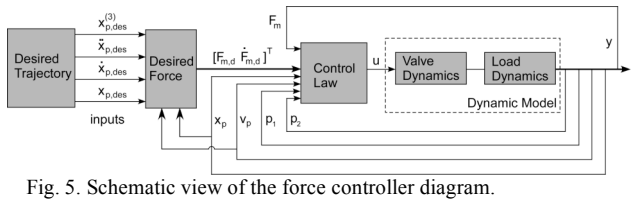

Fig. 5. Schematic view of the force controller diagram.

A custom-designed benchmark setup shown in Fig. 6 was built at the NTUA to test the proposed controller. The particular design of the setup allows for easy changes in the static and dynamic components of the inertial load, driven by the actuator. This is achieved by varying the angle of the cylinder with respect to the horizontal and by changing the cylinder inertia, by adding or removing load's weight.

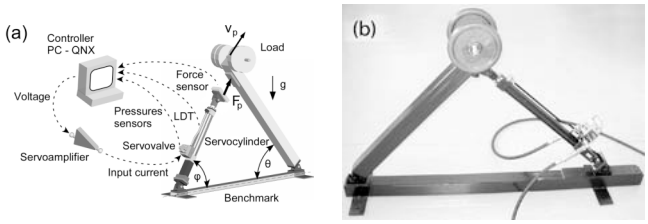

Fig. 6. (a) Schematic of control system setup and benchmark, (b) The real driven load and its servomechanism.

A Moog G122-202A1 Series controller is used to read servocylinder headside and rodside pressure using pressure sensors on the valve manifold and piston rod position, from a built-in analog LDT. A force cell at the end of the rod will provide the load force. To use nonlinear and model based controllers, the PID control section of the card will be by passed and the card will be used only for reading feedback measurements and for sending the appropriate control voltages to the servoamplifier. The servoamplifier in turn will send appropriate currents to the servovalve.

C. Simulation Results

The tracking performance of the controller is evaluated on the full hydraulic servosystem, described by (15a-h), using Matlab/Simulink. System parameters include the load supportive beam mass and inertia, $m_1 = 15.11\,\text{kg}$, $I_1 = 6.32\,\text{kgm}^2$ and geometrical parameters such as $r_1 = 1.04\,\text{m}$, $r_2 = 0.08\,\text{m}$ and $r_3 = 1.64\,\text{m}$, see Fig. 2. Friction parameters are $b = 200\ \text{Ns/m}$, $F_{c0} = 50\ \text{N}$, $F_{s0} = 20\ \text{N}$. The desirable trajectory of the load is given by

$$x_{p,des} = x_{01} + x_0 \cos(\omega t) \tag{26}$$

where $x_{01}\,[m]$ and $x_0\,[m]$ are trajectory constants, $\omega = 2\pi f\ [\text{rad/s}]$ is the angular velocity and $f\,[\text{Hz}]$ is the frequency of piston excitation.

Simulations runs were obtained using a number of desirable trajectories. As an example, Fig. 7 shows typical results, in which the desired trajectory is given by (26) with $m = 80\,\text{kg}$, $f = 0.1\,\text{Hz}$, $x_{01} = 0.3\,\text{m}$, $x_0 = 0.1\,\text{m}$ and $K_v = 180$, $K_p = 8.2\times10^3$ and $K_f = 6.5\times10^3$.

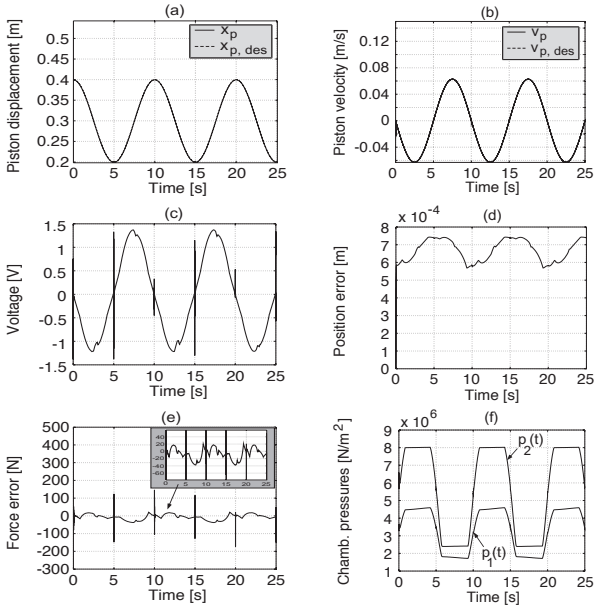

Fig. 7. Simulation results. (a) Piston displacement response, (b) Piston velocity response, (c) Input signal, (d) Position error history, (e) Force error history, (f) Chamber pressures histories.

The piston displacement and velocity responses, the input signal, the position and force history errors, as well as chamber pressures histories are shown in Fig. 7. The force error converges to zero, as was expected, in time $t_{s,f} = K_f^{-1}$. Further, it is obvious that the position error converges to zero in time $t_{s,x} = 6\,K_p^{-1/2}$, as was expected. The remaining position and force errors of the steady state are due to the inertial forces caused by the harmonic trajectory. The peaks observed are due to opening or closing of the valve and are of numerical nature. Future work includes interfacing a controller card to a PC running the QNX RTOS and materializing the developed controller.

IV. Conclusions

In this paper, a tracking controller for electrohydraulic servosystems based on a fast model-based force tracking loop was developed. The rigid body equations of motion and the hydraulic dynamics were integrated to form the

system dynamics. Friction and leakage of hydraulic elements were included in the full electrohydraulic model. The control analysis was based on a non-linear input-output linearization control approach. The control law was includes a PD part driving the tracking error to zero exponentially. A case study using a one degree of freedom servomechanism was presented. Simulations with typical desired trajectories were presented and a good performance of the controller was obtained. The approach can be further extended to hydraulic manipulator and simulator control.

APPENDIX

The equation of motion for the mechanical load is derived applying the Lagrange formulation given by (12). To this end, the Lagrangian is given by

$$L = K - V \tag{A1}$$

where K and V are the total kinetic and potential energy of the servosystem respectively, which are given by

$$K = [I_{\text{eq,L}}\dot{\varphi}^2 + m_p\dot{x}_p^2 + I_{\text{eq},act}\dot{\theta}^2]/2 \tag{A2a}$$

$$V = [(r_1 + r_2)m_{\text{eq,L}}\sin\varphi + (x_{\text{p}}m_{\text{p}} + \Lambda_{\text{eq},act})\sin\theta]g \tag{A2b}$$

where x_{p} is actuator displacement, g is the acceleration of gravity, φ, θ, r_1 and r_2 are defined in Fig. 2, $I_{\text{eq,L}}$ is the equivalent load moment of inertia, which includes the load and the load supportive beam moments of inertia, about their centers of mass, $I_{\text{eq},act}$ is the equivalent actuator moment of inertia, which contains the cylinder and piston moments of inertia, about their centers of mass, is the piston mass, $m_{\text{eq,L}}$ is the equivalent load mass, which includes the load mass and the load mass of the supportive beam mass and $\Lambda_{\text{eq},act}$ is the sum of the products of the actuator masses times actuator lengths, which includes the cylinder and piston masses and cylinder and piston lengths.

In (12), $M(x_{\text{p}})$, $G(x_{\text{p}})$ and $V(x_{\text{p}}, \dot{x}_{\text{p}})$ are given by

$$\begin{aligned} M(x_{\text{p}}) = {} & m_p + x_{\text{p}}^2 I_{\text{eq,L}}(r_1 r_2)^{-2}\csc^2\varphi \\ & + (x_{\text{p}}\csc\theta - r_3\cot\theta)^2(x_{\text{p}}r_3)^{-2}I_{\text{eq},act} \end{aligned} \tag{A3a}$$

$$\begin{aligned} G(x_{\text{p}}) = {} & g[x_{\text{p}}(r_1 + r_2)(r_1 r_2)^{-1}m_{\text{eq},L}\cot\varphi + m_{\text{p}}\sin\theta - \\ & -(x_{\text{p}} - r_3\cos\theta)\cdot(x_{\text{p}}r_3)^{-1}(x_{\text{p}}m_{\text{p}} + \Lambda_{\text{eq},act})\cot\theta] \end{aligned} \tag{A3b}$$

$$\begin{aligned} V(x_{\text{p}}, \dot{x}_{\text{p}}) = {} & \{(x_{\text{p}}m_{\text{p}} + \Lambda_{\text{p}})(x_{\text{p}} - r_3\cos\theta)^2 \\ & (x_{\text{p}}r_3)^{-2}\csc^2\theta - x_{\text{p}}I_{\text{eq,L}}\csc^4\varphi\cdot \\ & (x_{\text{p}}^2\cos\varphi - r_1 r_3\sin^2\varphi)(r_1 r_3)^{-2} + \\ & I_{\text{eq},act}(x_{\text{p}}r_3)^{-3}\{[(x_{\text{p}} - r_3\cos\theta)\cdot \\ & \cdot\csc^2\theta(x_{\text{p}}r_3 - r_3^2\cos\theta - x_{\text{p}}r_3\cdot \\ & \cot^2\theta + x_{\text{p}}^2\cot\theta\csc\theta) - r_3\csc\theta\cdot \\ & (x_{\text{p}}\csc\theta - r_3\cot\theta)(2x_{\text{p}} - 2r_3\cdot \\ & \cos\theta + x_{\text{p}}\cot^2\theta - r_3\cot\theta\csc\theta)]\}\}\dot{x}_{\text{p}}^2 \end{aligned} \tag{A3c}$$

where r_3 is defined in Fig. 2 and Λ_{p} is the product of the piston mass times piston length.

REFERENCES

[1] K. Six, T. A. Lasky, and B. Ravani, "A Time-Delayed Dynamic Inversion Scheme for Mechatronic Control of Hydraulic Systems," *IEEE/ASME Int. Conf. on Advanced Intelligent Mechatronics Proc.*, Como, Italy, 2001, pp. 1232–1238.

[2] M. Jelali, and A. Kroll, *Hydraulic Servo-systems. Modelling, Identification and Control*, Springer, 2003.

[3] D. Garagic, and K. Srinivasan, "Application of Nonlinear Adaptive Control Techniques to an Electrohydraulic Velocity Servo-mechanism," *IEEE Trans. on Control Systems Tech.*, vol. 12, No. 2, 2004, pp. 303–314.

[4] M. R. Sirouspour, and S. E. Salcudean, "Nonlinear Control of Hydraulic Robots," *IEEE Trans. on Robotics and Automation*, vol. 17, No. 2, 2001, pp. 173–182.

[5] N. Niksefat, and N. Sepehri, "Robust Force Controller Design for an Electro-Hydraulic Actuator Based on Nonlinear Model," *Proc. 1999 IEEE Int. Conf. Robotics & Automation*, San Francisco, pp. 200–206.

[6] B. Daachi, A. Benallegue, and N. K. M'Sirdi, "A Stable Neural Adaptive Force Controller for a Hydraulic Actuator," *Proc. 2001 IEEE Int. Conf. Robotics & Aut.*, Seoul, Korea, pp. 3465–3470.

[7] L. Laval, N. K. M'Sirdi, and J. C. Cadiou, "H_∞-Force Control of a Hydraulic Servo-Actuator with Environmental Uncertainties," *Proc. 1996 IEEE Int. Conf. on Robotics & Automation*, Minneapolis, Minnesota, pp. 1566–1571.

[8] S. Tafazoli, S. E. Salcudean, K. H. Zaad, and P. D. Lawrence, "Impedance Control of a Teleoperated Excavator," *IEEE Trans. on Control Systems Tech.*, vol. 10, No. 3, 2002, pp. 355–367.

[9] D. W. Robinson, and G. A. Pratt, "Force Controller Hydro-Elastic Actuator," *Proc. 2000 IEEE Int. Conf. on Robotics & Automation*, San Francisco, pp. 1321–1327.

[10] R. Liu, and A. Alleyne, "Nonlinear Force/Pressure Tracking of an Electro-Hydraulic Actuator," *Trans. of the ASME*, vol. 122, 2000, pp. 232–237.

[11] A. G. Alleyne, and R. Liu, "Systematic Control of a Class of Nonlinear Systems with Application to Electrohydraulic Cylinder Pressure Control," *IEEE Trans. on Control Systems Tech.*, vol. 8, No. 4, 2000, pp. 623–634.

[12] G. A. Sohl, and J. E. Bobrow, "Experiments and Simulations on the Nonlinear Control of a Hydraulic Servosystem," *IEEE Trans. on Control Systems Tech.*, vol. 7, No. 2, 1999, pp. 238–247.

[13] M. Honegger, and P. Corke, "Model-Based Control of Hydraulic Actuated Manipulators," *Proc. 2001 IEEE Int. Conf. on Robotics & Automation*, Seoul, Korea, pp. 2553–2559.

[14] P. Chatzakos, and E. Papadopoulos, "On Model-Based Control of Hydraulic Actuators," *Proc. of RAAD'03, 12th Int. Workshop on Robotics*, 2003.

[15] J. J. E. Slotine, and W. Li, *Applied Nonlinear Control*, Prentice Hall, 1991.

[16] H. E. Merritt, *Hydraulic Control Systems*, J. Wiley, 1967.

[17] B. A. Helouvry, P. Dupont, and C. C. De Wit, "A Survey of Models, Analysis Tools and Compensation Methods for the Control of Machines with Friction," *Automatica,* 30: 7, 1994, pp. 1083-1138.

[18] D. Stewart, "A platform with six degrees of freedom," *Proc. of the IMechE*, Vol. 180, Pt. 1, No 15, 1965-66, pp. 371-385.